

# Study of Propylene Glycol and Dimethylformamide Vapors Sensors Based on MWCNTs/SnO<sub>2</sub> Nanocomposites

Zaven Adamyan, Artak Sayunts, Vladimir Aroutiounian, Emma Khachatryan, Arsen Adamyan  
Yerevan State University, Department of Physics of Semiconductors and Microelectronics  
YSU  
Yerevan, Armenia  
e-mail: kisahar@ysu.am

Martin Vrnata, Přemysl Fitl, Jan Vlček  
University of Chemistry and Technology, Department of Physics and Measurement Technology  
UCT  
Prague, Czech Republic  
e-mail: martin.vrnata@vscht.cz

**Abstract**—We present results of our research works related to the study of thick-film multiwall carbon nanotube/tin oxide nanocomposite sensors of propylene glycol (PG) and dimethylformamide (DMF) vapors derived using hydrothermal synthesis and sol-gel methods. Investigations of response/recovery characteristics in the 50-300°C operating temperature range reveal that the optimal operating temperature for PG and DMF vapor sensors, taking into account both high response and acceptable response and recovery times, are about 200 and 220°C, respectively. A sensor response dependence on gas concentration in both cases is linear. The minimal propylene glycol and dimethylformamide gas concentrations at which the perceptible signal was registered by us were 13 ppm and 5 ppm, respectively.

**Keywords**—MWCNTs/SnO<sub>2</sub>; gas; vapor; sensor; dimethylformamide; propylene glycol.

## I. INTRODUCTION

There are various harmful and hazardous matter vapors, which have a major role in diverse spheres such as environmental protection, industrial manufacture, medicine, as well as national defense. As an illustration, propylene glycol (PG) is an excellent solvent for many organic compounds and is used as an active ingredient in engine coolants and antifreeze, brakes, paints, enamels and varnishes, and in many products as a solvent or surfactant. It can also be found in cosmetics, perfumes, as well as in pharmaceuticals.

Another example is the dimethylformamide (DMF) which is used as a solvent in vinyl resins, adhesives, pesticide and epoxy formulations; which purifies and separates of acetylene, 1,3-butadiene, acid gases and aliphatic hydrocarbons, also in the production of polyacrylic or cellulose triacetate fibres and pharmaceuticals or in the production of polyurethane resin for synthetic leather [3].

DMF and PG have a huge impact on human organs (e.g. liver, skin, eyes and kidneys [1]-[3]). PG can cause nausea and vomiting, headache, dizziness and fainting. Moreover, it is known as a combustible liquid, which can explode in fire.

Due to the information noted above, PG and DMF gas sensors have a huge application for detecting and continuous monitoring of these gases, in the spheres where they are used. As a result of our carefully conducted analysis of the

literature data, we did not find any works related to research and development of resistive sensors of PG and DMF gases. There are only sensors working in other principle (for example sensors working on modification of color of the substance), which is incompatible for contemporary technic, while, resistive gas sensors made from metal oxides have advantages such as electric signal, measurement of concentration, small sizes, low power consumption, high sensitivity, and long reliability [4]-[6].

Nanomaterials, as carbon nanotubes (CNTs), metal-oxide nanoparticles, nanotubes, nanowires and other various nanopatterns formation [7]-[12] are widely used in gas sensings for their excellent responsive characteristics, mature preparation technology, and low cost of mass production. Due to the covering of CNTs walls with metal-oxide nanoparticles, specific surface area of such gas-sensitive nanocomposites increases more. Moreover, nanochannels in the form of hollows of CNTs promote penetration of gas molecules deeper down in the nanocomposite sensitive layer [13]. Hence, it can be expected that application in gas sensors technology of nanocomposite structures composed of metal oxide functionalized with CNTs should enhance the gas sensor parameters, such as gas response, response, recovery times, and operating temperatures.

Our recent works related to the study of gas sensors based on multiwall carbon nanotubes/tin oxide (MWCNTs/SnO<sub>2</sub>) nanostructures are also argued in [10] [14] [15]. The choice of tin oxide as a component of SnO<sub>2</sub>/MWCNTs nanocomposite structure is conditioned by the fact that SnO<sub>2</sub> is well known and studied basic material for metal-oxide gas sensors (see, for example [4] [9] [16] [17]). We expected that coating of functionalized MWCNTs with SnO<sub>2</sub> nanoparticles with admissible, (close to double Debay length) sizes [16]-[20] should provide the improved performance of the gas sensor and lowered temperature of its operating

Here, we present the characteristics of the PG and DMF vapor sensors based on ruthenated thick-films MWCNT/SnO<sub>2</sub> nanocomposite structures. The choice of corresponding processing technique, treating conditions and regimes for CNTs functionalization, as well as modification of thick films surface with Ru catalyst, are described below in the second section. Results of the measurements of PG

and DMF vapor sensors and their discussions are given in the third section.

## II. EXPERIMENTAL DEVELOPMENT

MWCNTs/SnO<sub>2</sub> nanocomposite material processing and thick-film sensor manufacturing technology on the base of this nanocomposite are presented in this section. It is shortly described both the MWCNTs preparation and its covering with SnO<sub>2</sub> nanoparticles obtained by using the hydrothermal method. Ruthenium catalyst deposition technology is also shown here.

### A. Material preparation

Firstly, MWCNTs were prepared by the decomposition of acetylene (CVD method) using Fe, Co/CaCO<sub>3</sub> catalyst [21] [22]. Such growth procedure using CaCO<sub>3</sub> catalyst enables a highly efficient selective formation of clean MWCNTs, suitable for effective bonding between CNT and metal-oxide, particularly, for SnO<sub>2</sub> precursors.

The preparation of nanocomposite materials with a hydrothermal method was carried out in two steps. Firstly, purified MWCNTs were dispersed in water via sonication. Then, a calculated amount of precursor of the SnCl<sub>2</sub>·2H<sub>2</sub> was dissolved in another beaker in water, whereupon 3 cm<sup>3</sup> HCl was added to the solution. In the next step, the MWCNT's suspension and the solution of the precursor were mixed and sonicated for 30 min. For preparing the nanocomposites, we poured the above-mentioned solutions into autoclaves, where hydrothermal synthesis was carried out at 150°C for 1 day. At the end of this procedure, all obtained nanocomposite powders were filtered and dried at 90°C for 5h. The final mass ratios of the nanocomposite MWCNT/SnO<sub>2</sub> obtained with the hydrothermal method in this study were 1:200, respectively. The hydrothermal synthesis process is presented in details in [10] [23].

### B. Samples

The paste for the thick film deposition made by mixing powders with  $\alpha$ -terpineol ("Sigma Aldrich") and methanol was printed on the chemically treated surface of the alumina substrate over the ready-made Pt interdigitated electrodes. The thin-film Pt heater was formed on the back side of the substrate. Then, the obtained composite structures were cut into 3×3 mm pieces. After that, the drying and annealing processes of the resulting thick films were carried out in two stages: The first step is the heating of thick films up to 220°C with 2°C×min<sup>-1</sup> rate of temperature rise and holding for 3h and then increasing in temperature until 400°C with 1°C×min<sup>-1</sup> rate and holding for 3h. In the second step, the thick-film specimens were cooled down in common with the oven.

After annealing and cooling processes, the surface of MWCNTs/SnO<sub>2</sub> thick films was ruthenated by dipping samples into the 0.01M RuOHCl<sub>3</sub> aqueous solution for 20min whereupon drying at 80°C for 30 min. Then, the annealing treatment was carried out again by the same method noticed above. The choice of the ruthenium as a catalyst was determined by its some advantages [10] [15] [23]. At the final stage, ruthenated MWCNT/SnO<sub>2</sub> chips

were arranged in TO-5 packages and the gas sensors would be ready to measurements after bonding of leads.

## III. RESULTS AND DISCUSSIONS

Some results of the nanocomposite surface morphology study, as well as gas sensor characteristics, are shown in this section, but the performances of PG and DMF sensors are separately considered. Also, the dependence of electrical resistance of the sensors on operating temperature, as well as values of responses, response and recovery times of the sensors at various operating temperatures or target gas concentrations are shown here too.

### A. Material characterization

The morphologies of the prepared SnO<sub>2</sub>/MWCNT nanocomposite powders with diverse compounds were studied by scanning electron microscopy using Hitachi S-4700 Type II FE-SEM equipped with a cold field emission gun operating in the range of 5–15kV. The presence of an oxide layer was confirmed by SEM-EDX. Furthermore, the crystalline structure of the inorganic layer was also studied by an X-ray diffraction method using the Rigaku Miniflex II diffractometer (angle range: 2 $\theta$  [°]=10–80 utilizing characteristic X-ray (CuK $\alpha$ ) radiation). Results of these investigations were presented in [10] [23] more detailed. Here, we are only noting that average crystalline size of SnO<sub>2</sub> nanoparticles estimated from SEM images and XRD patterns are less than 12 nm but the average diameter of non-covered by SnO<sub>2</sub> nanoparticles CNTs was about 40 nm.

### B. Gas sensing characteristics

Gas sensing properties of the MWCNTs/SnO<sub>2</sub> nanocomposite structures were measured by home-made developed and computer-controlled static gas sensor test system [20]. The sensors were reheated and studied at different operating temperatures. When the electrical resistance of all studied sensors was stable, the vital assigned amount of compound in the liquid state for sensors testing was injected by a microsyringe in measurement chamber. Moreover, the target matters were introduced into the chamber on the special hot plate designed for the quick conversion of the liquid substance to its gas phase. After its resistance reached a new constant value, the test chamber was opened to recover the sensors in air. The sensing characteristics were studied in the 20–300°C operating temperature range and the gas response of the sensors determines as  $R_a/R_g$  where  $R_a$  and  $R_g$  are the electrical resistances in the air and in target gas-air atmosphere, respectively. The response and recovery times are determined as the time required for reaching the 90% resistance changes from the corresponding steady-state value of each signal.

### C. PG vapor sensor characteristics

Firstly, we should determine the operating temperature of the sensors. As a result of measurements of the sensor resistance in air and air/gas environment, the maximal response to 650 ppm PG vapor was revealed at 200°C operating temperature (Figure 1 and Figure 2).

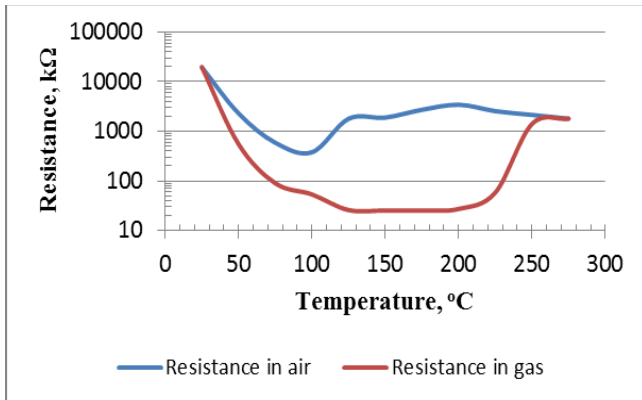


Figure 1. Dependence of electrical resistance change of MWCNTs/SnO<sub>2</sub> thick-film sensors on operating temperature.

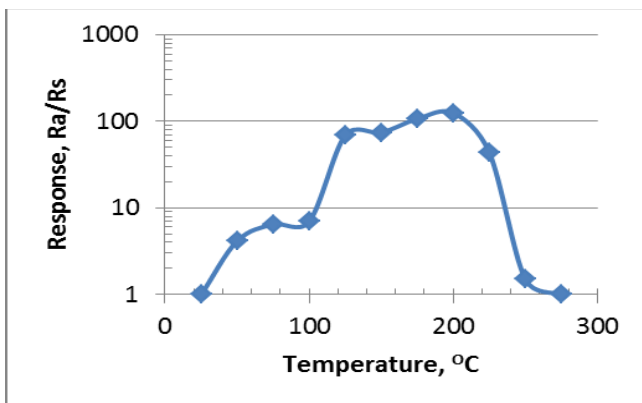


Figure 2. Response of MWCNTs/SnO<sub>2</sub> thick-film PG sensors vs operating temperature.

Good repeatability of the sensor response can be seen from Figure 3, where the electrical resistance change of PG sensor vs. time measured upon cyclic exposure of 650 ppm PG vapors in air at 200°C operating temperature is presented.

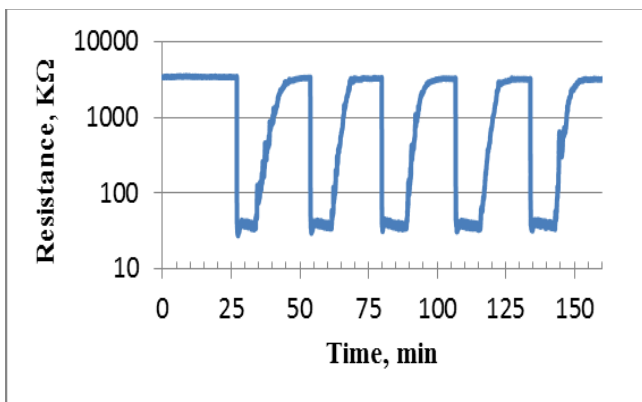


Figure 3. The electrical resistance change of MWCNTs/SnO<sub>2</sub> thick-film PG sensors vs time measured upon cyclic exposure of 650 ppm PG vapors in air at 200°C operating temperature.

Changes of the response of PG vapor sensor, as well as the response and recovery times depending on operating temperature, are shown in Table I. Pursuant to the Table I,

maximal response to PG vapor ( $R_a/R_g=125$ ) was fixed for about 5s at 200°C operating temperature, but recovery process takes place sufficiently slowly at this temperature. At higher operating temperatures, the recovery of the sensor parameters occurs for a considerably short time, but the response of the sensor decreases noticeably.

TABLE I. CHANGES OF THE 650 PPM PG VAPOR SENSOR RESPONSE AND RESPONSE AND RECOVERY TIMES AT DIFFERENT OPERATING TEMPERATURES.

Operating temperature, °C	Response, $R_a/R_g$	Response time, s	Recovery time, min
75	6.56	1300	100
100	7	159.6	56
125	6.2	28.8	45
150	37.8	9	11.6
175	107.1	6	21
200	125	170	10
225	43.7	6	0.83
250	1.5	3.96	0.1

Dependence of the resistance and response of MWCNTs/SnO<sub>2</sub> sensor on PG vapor concentration is shown in Figure 4 and Figure 5, respectively. As it is obvious from the figures, the sensor response occurs down to small target gas concentrations (15 ppm) but the response approximately linearly depends on the gas concentration.

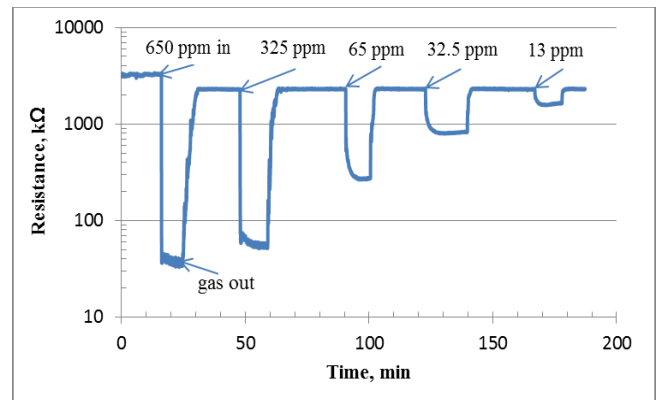


Figure 4. The response/recovery curves observed at different PG concentrations exposure measured at 200°C operating temperature.

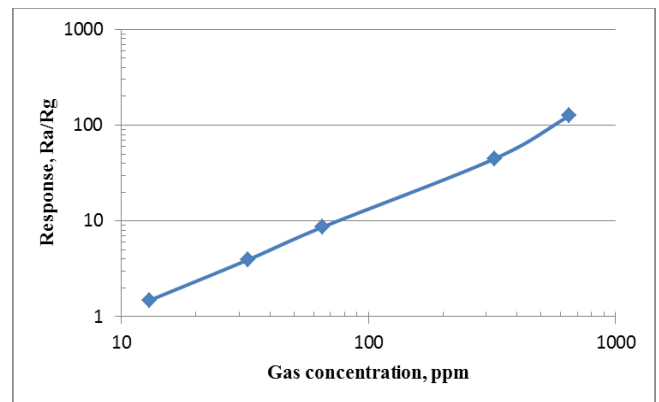


Figure 5. Dependence of the response of MWCNTs/SnO<sub>2</sub> PG vapor sensor on gas concentration measured at 200°C operating temperature.

D. DMF vapor sensor characteristics

The sensor response derived as a result of 500 ppm DMF vapor exposure versus operating temperature is presented in Figure 6. It can be seen that maximal response, in this case, is registered in the range of 210-225°C. Taking into account, a relatively high response, shorter response and also recovery times (see Table II), are demonstrated at 225°C operating temperature.

Dependence of the sensor response on versus DMF vapor concentration is also linear (Figure 7).

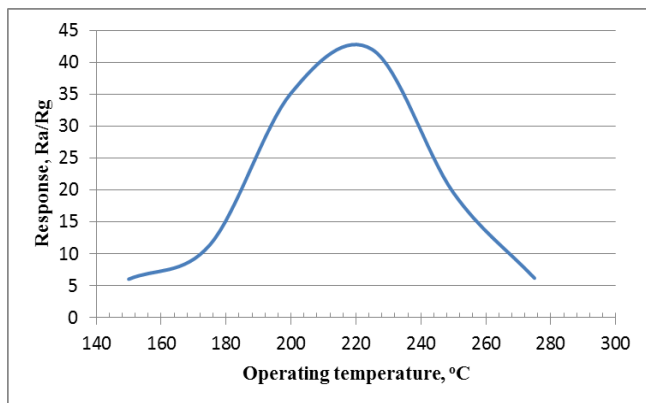


Figure 6. Response vs operating temperature at 500 ppm DMF vapor exposure.

TABLE II. CHANGES OF THE 500 PPM DMF VAPOR SENSOR RESPONSE AND RESPONSE AND RECOVERY TIMES AT DIFFERENT OPERATING TEMPERATURES.

Operating Temperature, °C	Response, Ra/Rg	Response time, s	Recovery time, s
150	6.03	90	330
175	11.42	12	240
200	35.2	6	210
225	42.04	5	50
250	19.6	4	6
275	6.2	4	1

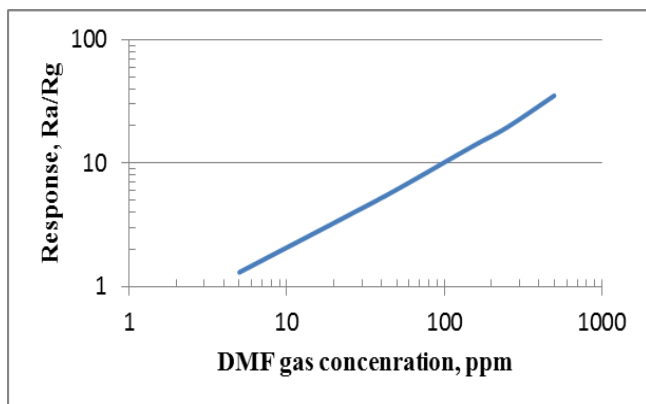


Figure 7. The sensor response vs 500 ppm DMF vapor concentration measured at 200°C operating temperature.

E. On possible mechanism of gas sensitivity

It is known that the attachment of carboxyl groups on the surface of MWCNTs is effective in nucleation and trapping

the other materials including tin oxide nanoparticles. As it was shown earlier, COOH groups attached on the surface of MWCNTs have a strong interaction with alcohol vapors resulting hydrogen bond between COOH groups and the OH groups of alcohol molecules [10] [15]. This hydrogen bond should be removed by increasing the temperature, which contributes to long recovery times in MWCNTs/SnO<sub>2</sub> sensors.

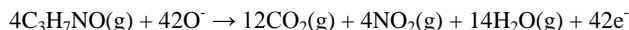
The higher operating temperature of the gas response is observed until it reaches its maximal value. With the subsequent increase in operating temperature, desorption of chemisorbed oxygen ions takes place and gas response decreases; the recovery time decreases, too.

MWCNTs nanochannels play a smaller role at relatively more content of SnO<sub>2</sub> in the nanocomposite (as in our case), as nanotubes are closed by plenty of SnO<sub>2</sub> nanoparticles. Due to it, accessibility of gas molecules penetration to MWCNTs nanochannels through the metal-oxide thick film is very difficult. Therefore, the gas response is mainly determined by a number of metal-oxide nanoparticles and a considerable amount of surface adsorption sites. MWCNTs only prevent the formation of agglomerates of SnO<sub>2</sub> and ensure the development of the surface because of repulsive forces between the carboxyl groups adsorbed on it.

The oxidation reaction of PG and DMF vapors on the nanocomposite surface could be represented as follows, respectively:



and



At the temperature corresponding to the highest response, the reactivity of the target gas molecules is proportional to the speed of diffusion into the sensing layer. Hence, the target gas has the chance to sufficiently penetrate into the sensing layer and react with an appropriate speed. The competition between the amount of adsorbed target gases and their oxidation rate supports the maximum response and its sharp decline. With the following increase in operating temperature, desorption of the adsorbed oxygen ions from the surface of the sensor is increased. It follows that less amount of oxygen ions presents on the surface of SnO<sub>2</sub>, might take part in reaction with target gases at higher operating temperature. Therefore, the response falls at high operating temperatures. Furthermore, it influences the physical properties of the semiconducting sensor material. For instance, at higher temperatures the carrier concentration increases (resulting from the release of electrons back to the conduction band in consequence of desorption of adsorbed oxygen) and the Debye length decreases. This may also be one of the possible reasons for the rise in R<sub>g</sub> curve in Figure 1, which leads to the decrease in response at higher temperatures.

Although molecular weights of both considered target gases are close to each other, the quantity of carbon atoms is

the same. Nevertheless, the response from DMF vapors influences less due to many adsorbed oxygen ions, resulted from the chemical decomposition, which demands for the full oxidation reaction. Thus, the 1:200 weight ratios of the nanocomposite sensor components with relatively large amount of SnO<sub>2</sub> particles promote an initiation of a sufficiently large quantity of ionized adsorption centers, which ensure relatively high response to DMF gas exposure.

As for selectivity, this nanocomposite sensor demonstrates cross-sensitivity to some alcohols, such as butanol, methanol and ethanol at 200°C operating temperature. Moreover, it influences by other gases, and as a rule, does not facilitate the formation of noticeable gas response at 200°C operation temperature. A sufficiently large signal is possible to obtain at higher operating temperatures, at which developed sensor does not react to diverse impacts of PG and DMF gases. For instance, the sensor exhibits a high response to toluene vapor only around of 250°C operating temperature [14] [23].

Unlike existing other type PG and DMF sensors, presented nanocomposite sensor is able to measure the concentration of mentioned gases in the atmosphere.

#### IV. CONCLUSION

In this paper, we have carried out the investigation of obtaining ruthenated MWCNTs/SnO<sub>2</sub> thick-film nanocomposite sensors using hydrothermal synthesis and sol-gel technologies. It is revealed that studied sensors give a sufficiently high response to such harmful and hazardous gases as PG and DMF at relatively low operating temperatures. The fast response of the sensors (at the order of seconds) and acceptable recovery times are observed under all gas concentrations influence at 200°C operating temperature. The minimal PG and DMF gas concentrations at which the perceptible signal is registered are 13 ppm and 5 ppm, respectively.

Due to the linear dependence of the response on the concentration of target gas, it is possible to easily measure the concentration of mentioned gases in the atmosphere.

#### ACKNOWLEDGMENT

This work was supported by NATO EAP SFPP 984.597.

#### REFERENCES

- [1] G. Malaguamera et al. "Toxic hepatitis in occupational exposure to solvents", *World J. Gastroenterol.* Vol. 18(22), pp. 2756–2766, 2012; doi: 10.3748/wjg.v18.i22.2756v
- [2] H. Y. Chang, T. S. Shih, Y. L. Guo, C. Y. Tsai, and P. C. Hsu, "Sperm function in workers exposed to N,N-dimethylformamide in the synthetic leather industry", *Fertil Steril.* Vol. 81(6), pp. 1589-1594, 2004. DOI: 10.1016/j.fertnstert.2003.10.033
- [3] A. Fiorito, F. Larese, S. Molinari, and T. Zanin, "Liver function alterations in synthetic leather workers exposed to dimethylformamide", *American journal of industrial medicine* vol. 32, pp. 255-260, 1997.
- [4] V. M. Aroutiounian, "Use of Metaloxide, porous silicon and carbon nanotube gas sensors for safety and security, in *Advanced Sensors for Safety and Security*", A. Vaseashta, S. Khudaverdyan, eds., NATO Science for Peace and Security, Series B: Physics and Biophysics, Chapter 9, 2012.
- [5] G. F. Fine, L. M. Cavanagh, A. Afonja, and R. Binions, "Metal oxide semi-conductor gas sensors in environmental monitoring", *Sensors* v. 10, pp. 5469-5502, 2010; doi:10.3390/s100605469.
- [6] G. Korotcenkov, S. H. Han, and B. K. Cho, "Material design for metal oxide chemiresistive gas sensors", *J. of Sensor Science and Technology*, vol. 22, pp. 1-17, 2013; http://dx.doi.org/10.5369/JSST.2013.22.1.1.
- [7] V. M. Aroutiounian, "Gas sensors based on functionalized carbon nanotubes", *Journal of Contemporary Physics (Armenian Academy of Sciences)*, vol. 50, pp. 333–354, 2015; *Izvestiya NAN Armenii, Fizika*, vol. 50, pp. 448–475, 2015; DOI: 10.3103/S1068337215040064
- [8] M. M. Arafat, B. Dinan, S. A. Akbar, and A. S. M. A. Haseeb, "Gas sensors based on one dimensional nanostructured metal-oxides: A Review", *Sensors*, vol. 12, pp. 7207-7258, 2012; doi:10.3390/s120607207.
- [9] G. Korotcenkov, S.-D. Han, B. K. Cho, and V. Brinzari, "Grain size effects in sensor response of nanostructured SnO<sub>2</sub>- and In<sub>2</sub>O<sub>3</sub>-based conductometric thin film gas sensor", *Critical Reviews in Solid State and Materials Sciences* vol. 34, pp. 1–17, 2009; doi: 10.1080/10408430902815725.
- [10] V. M. Aroutiounian et al. "Study of the surface-ruthenated SnO<sub>2</sub>/MWCNTs nanocomposite thick-film gas sensors", *Sensors and Actuators B* vol. 177, pp. 308–315, 2013; doi: org/10.1016/j.snb.2012.10.106.
- [11] S. A.-Feyzabad, A. A. Khodadadia, M. V.-Naseh, and Y. Mortazavi, "Highly sensitive and selective sensors to volatile organic compounds using MWCNTs/SnO<sub>2</sub>", *Sensors and Actuators B* vol. 166–167, pp. 150–155, 2012; doi: 10.1016/j.snb.2012.02.024.
- [12] N. V. Hieu, L. T. B. Thuy, and N. D. Chien, "Highly sensitive thin film NH<sub>3</sub> gas sensor operating at room temperature based on SnO<sub>2</sub>/MWCNTs composite", *Sensors and Actuators B* vol. 129 pp. 888–895, 2008; doi:10.1016/j.snb.2007.09.088.
- [13] X. Bai, H. Ji, P. Gao, Y. Zhang, and X. Sun, "Morphology, phase structure and acetone sensitive properties of copper-doped tungsten oxide sensors", *Sens. Actuators B* vol. 193, pp. 100–106, 2014; doi: org/10.1016/j.snb.2013.11.059.
- [14] V. M. Aroutiounian, Z. N. Adamyan, A. G. Sayunts, E. A. Khachaturyan, and A. Z. Adamyan, "Study of MWCNT/SnO<sub>2</sub> nanocomposite acetone and toluene vapor sensors", *Proc. of 17 Int. Conf. on Sensors and Measurement Technology, SENSOR 2015*, May 19-21, Nierenberg, Germany, pp. 836-841, 2015. DOI 10.5162/sensor2015/P8.3.
- [15] Z. N. Adamyan, A. G. Sayunts, E. A. Khachaturyan, and V. M. Aroutiounian, "Study of nanocomposite thick-film butanol vapor sensors", *Journal of Contemporary Physics (Armenian Academy of Sciences)*, vol. 51(2), pp. 143-149, 2016 *Izvestiya NAN Armenii, Fizika*, vol. 51, pp. 448–475, 2015; DOI: 10.3103/S1068337216020067;.
- [16] V. M. Aroutiounian, "Metal oxide hydrogen, oxygen, and carbon monoxide sensors for hydrogen setups and cells", *Int. J. of Hydrogen Energy* vol. 32(9), pp. 1145–1158, 2007.
- [17] P. Shankar, J. Bosco, and B. Rayappan, "Gas sensing mechanism of metal oxides: The role of ambient atmosphere, type of semiconductor and gases - A review", *Sci. Lett.*, vol. 4: 126, pp. 1-18, 2015.
- [18] C. Xu, J. Tamaki, N. Miura, and N. Yamazoe, "Grain size effects on gas sensitivity of porous SnO<sub>2</sub>-based elements", *Sensors and Actuators B* vol. 3 pp. 147–155, 1991.
- [19] A. Z. Adamyan, Z. N. Adamyan, and V. M. Aroutiounian, "Preparation of SnO<sub>2</sub> films with thermally stable nanoparticles", *Sensors* vol. 3, pp. 438–442, 2003.
- [20] A. Z. Adamyan, Z. N. Adamyan, V. M. Aroutiounian, and A. H. Arakelyan, J. Turner, K. Touryan, "Sol-gel derived thin-

film semiconductor hydrogen gas sensor”, *Int. J. of Hydrogen Energy* vol. 32, pp. 4101–4108, 2007.

- [21] E. Couteau et al. “CVD synthesis of high-purity multiwalled carbon nanotubes using  $\text{CaCO}_3$  catalyst support for large-scale production,” *Chem. Phys. Lett.*, vol. 378, pp. 9-17, 2003.
- [22] A. Magrez, J. W. Seo, R. Smajda, M. Mionić, and L. Forró, “Catalytic CVD Synthesis of Carbon Nanotubes: Towards High Yield and Low Temperature Growth,” *Materials* vol. 3 pp. 4871-4891, 2010.
- [23] V. M. Aroutiounian et al. “Comparative study of VOC sensors based on ruthenated MWCNT/ $\text{SnO}_2$  nanocomposites”, *Int. J. of Emerging Trends in Science and Technology (IJETST)*, vol. 01/08, pp. 1309-1319, 2014: DOI :10.18535/ijetst.